



COB-2021-0791 INFLUENCE OF MESH STIFFNESS MODELING ON THE DYNAMIC RESPONSE OF GEARED ROTORS

Laís Bittencourt Visnadi

Hélio Fiori de Castro

School of Mechanical Engineering - University of Campinas, Brazil

lais.visnadi@fem.unicamp.br, heliofc@fem.unicamp.br

Abstract. Gear pair dynamics is widely studied and recent researches present complex models to this purpose. When considering rotor dynamics, the mesh stiffness is usually approximated, although this is an important source of vibration on the rotating system. This paper intends to evaluate the influence of different methods for estimating mesh stiffness on the rotor response. The considered methods were API, step function, sinusoidal function and variable cross section beam. Of these, the beam method is the most detailed and was considered the reference. The mean value of step and sinusoidal functions was the value provided by API method, although it was lower than the mean value of mesh stiffness calculated by beam method. Sinusoidal function tends to underestimate response and step function tends to overestimate it, especially for a helical gear pair and at response high frequencies. For constant rotational speed problems, computational cost does not justify using approximations and beam method is recommended. For variable rotational speed problems, considering a sinusoidal function with API mean value is an option for spur gear pairs and with beam method mean value is better for helical gear pairs.

Keywords: mesh stiffness, spur gear, helical gear, gear pair dynamics

1. INTRODUCTION

Mesh stiffness is a time-varying phenomenon, depending on the mesh force position along gear teeth in mesh and the number of teeth pairs in contact. API Standard for Rotordynamics (API (2005)) suggests a constant approximation for mesh stiffness. Classical works about geared rotordynamics, such as Kahraman and Singh (1991) Kahraman *et al.* (1992), Rao *et al.* (1998) and, Kubur *et al.* (2004) consider a constant mesh stiffness. This simplifies the problem, but causes a prejudice on the analysis of the the entire machine dynamic behavior.

Detailed papers about gear pair dynamics (for example, Yi *et al.* (2019) and Kim *et al.* (2010) take into account pressure angle variation due to changes on gears center distance) consider an approximation of the time-varying mesh stiffness (TVMS) by a simple step function, in which mesh stiffness high and low levels are associated to double and simple contact. In general, papers about geared rotordynamics model mesh stiffness as a sinusoidal function (Theodossiades and Natsiavas (2001) Shin and Palazzolo (2020)), with the periodicity of the mesh.

A more suitable model to calculate TVMS is the one that regards the gear tooth as a cantilever beam with variable cross section. Then, TVMS of the gear pair is calculated considering a series association of tooth stiffness and, in some cases, also the gear body stiffness. Finally, total TVMS is the sum of the pairs stiffness along time, since contact ratio must be greater than one.

However, depending on the complexity of the dynamic model of the pair, the inclusion of mesh stiffness detailed model may become computationally expensive. Since the model of a rotating machine is even more comprehensive than the model of the gear pair, to study the effects of simpler models of TVMS on the dynamic response of the rotor is important.

Few studies comparing the influence of different mesh stiffness calculation methods on the dynamic response of the machine were published. Cooley *et al.* (2016) compared the dynamic response of a gear pair considering two finite elements methods of mesh stiffness calculation: average and local slope of the mesh force - deflection curve. Meagher *et al.* (2010) evaluated the differences on the dynamic response of a gear pair caused by a finite elements mesh stiffness model and a lumped parameter mesh stiffness model, which was similar to the variable cross section beam model considered in the present paper. Hence, this work intends to compare the dynamic response of geared rotors, taking into account the most used ways in literature to calculate mesh stiffness: API (constant mesh stiffness), step function, sinusoidal function and variable cross section beam.

2. MESH STIFFNESS MODELS

In order to compare the dynamic responses of a rotating system, four methods of calculating mesh stiffness were considered: API (constant mesh stiffness), functions of mesh period (step function and sinusoidal function) and variable

cross section beam. These models are detailed in the following subsections.

2.1 API

API Standard related to rotordynamics (API (2005)) briefly considers the influence of gear sets on rotating machinery. Although it explains about the existence of an excitation at the mesh frequency and mentions that it is not purely sinusoidal, it says that, historically, the mesh stiffness is not considered in the rotor model.

It recommends that, if desired, the mesh stiffness may be included on the model as constant coefficients:

$$K_{xx} = K' \cos^2 \gamma; \quad (1)$$

$$K_{xy} = K' \sin \gamma \cos \gamma; \quad (2)$$

$$K_{yx} = K_{xy}; \quad (3)$$

$$K_{yy} = K' \sin^2 \gamma; \quad (4)$$

$$K' = C(L) \cos^2 \beta 10^6; \quad (5)$$

$$\gamma = (A \times \alpha) + B \quad (6)$$

where L is the net facewidth of the gear, in millimeters, β is the helix angle, in degrees, C is a constant, equal to 12,057, α is the normal pressure angle, in degrees, A is equal to 1 for downloaded rotors and -1 for uploaded rotors and B is equal to 90° for clockwise rotation or 270° for counter-clockwise rotation, looking into coupling end. The unit of the calculated stiffness is N/m.

There are no further details about this calculation suggested in this standard. Wygant, K., Robertson, C., Li, F. (2018) say that the API committee members told that these equations were provided by a gearing manufacturing company.

2.2 Functions of mesh period

The step function model for the time-varying mesh stiffness takes into account that it is a periodic excitation and that it varies according to the number of teeth in contact. Considering a gear pair with contact ratio (m_p) between 1 and 2 and mesh period (T_m), the higher mesh stiffness (k_{max}) will occur when 2 pairs of teeth are in contact, and this double contact will last $(m_p - 1) \cdot T_m$. In the remaining time of the mesh cycle, only one pair of teeth will be in contact, and the mesh stiffness will be lower (k_{min}) (Yi *et al.* (2019)):

$$k_m(t) = \begin{cases} k_{max}, & t \leq (m_p - 1) \cdot T_m \\ k_{min}, & t > (2 - m_p) \cdot T_m \end{cases} \quad (7)$$

The sinusoidal function model also considers the periodic characteristic of mesh stiffness and it is usually modeled as a Fourier series (Shin and Palazzolo (2020)):

$$k_m(t) = k_0 + \sum_{i=1}^{\infty} s_i k_0 \cos j \omega_m t - \phi_i \quad (8)$$

where ω_m is the mesh frequency, i.e. $\omega_m = 1/T_m$ and k_0 is the mesh stiffness mean value.

2.3 Variable cross section beam

As explained by Ma *et al.* (2014), this method is based on elastic mechanics and considers the relation between potential energy and stiffness. The total potential energy of a tooth subjected to an acting external force is the sum of its

bending (*b*), axial compressive (*a*), shear (*s*) and fillet foundation (*f*) potential energies. Considering the contact of two surfaces, which is the case of a gear pair in mesh, there is also a Hertzian energy (*h*).

Therefore, the stiffness of a teeth single pair teeth in mesh is:

$$k = \left(\frac{1}{k_{b1}} + \frac{1}{k_{a1}} + \frac{1}{k_{s1}} + \frac{1}{k_{f1}} + \frac{1}{k_{b2}} + \frac{1}{k_{a2}} + \frac{1}{k_{s2}} + \frac{1}{k_{f2}} + \frac{1}{k_h} \right)^{-1} \quad (9)$$

Bending, axial compressive and shear stiffness are calculated considering the gear tooth as a variable cross section beam. Fillet foundation stiffness is calculated considering the application of the contact force and gear body deformation. Since the contact force application changes as the gear rotates, teeth pair stiffness changes along contact. Double and single contact periods are also considered in this method.

In the case of helical gears, the same theory is used, but because of the helix angle, the tooth is modeled as a series of staggered spur gears with no elastic coupling, as explained on Wan *et al.* (2015). Another difference is that helical gear mesh contact length also changes with time, so it needs to be taken into account.

3. ROTOR SYSTEM MODEL

A finite element model, based on the one presented by Rao *et al.* (1998), was used in this paper. This model considers torsional motions but does not consider translational axial motion.

The system equation of motion is given by:

$$[M]\{\ddot{q}\} + ([G] + [C])\{\dot{q}\} + ([K] + k_m[K_m])\{q\} = \{F\} \quad (10)$$

where $[M]$ is the mass matrix, $[G]$ is the gyroscopic matrix, $[C]$ is the damping matrix, $[K]$ is the stiffness matrix, $[K_m]$ is the stiffness matrix associated to the mesh, $\{F\}$ is the external forces vector, k_m is the mesh stiffness and q is the vector of displacements. The over dot indicates time derivative. In order to obtain $[K_m]$, the equations of motion proposed by Kubur *et al.* (2004) were considered, neglecting equations of axial movement. Relative displacement at the gear mesh in normal direction to contact faces is:

$$p(t) = (y_p \sin(\psi) - y_g \sin(\psi) + z_p \cos(\psi) - z_g \cos(\psi) + r_{bp}\theta_{xg} + r_{bg}\theta_{xg}) \cos(\beta) + (r_{bp}\theta_{yp} \sin(\psi) + r_{bg}\theta_{yg} \sin(\psi) + r_{bp}\theta_{zp} \cos(\psi) + r_{bg}\theta_{zp} \cos(\psi)) \sin(\beta) \quad (11)$$

where y is the horizontal displacement, z is the vertical displacement, subscript p indicates pinion, subscript g indicates gear, θ indicates rotation, r_b is the base radius, β is the helix angle and ψ is the angle of the line of action with a vertical reference line.

Considering that, a stiffness matrix for the gear pair is obtained:

$$[K_{m_{pair}}] = k_m \cdot \begin{bmatrix} [K_{pp}] & [K_{pg}] \\ [K_{gp}] & [K_{gg}] \end{bmatrix} \quad (12)$$

$$[K_{pp}] = \begin{bmatrix} c^2(\beta) s^2(\psi) & c^2(\beta) sc(\psi) & r_{bp} sc(\beta) s^2(\psi) & r_{bp} sc(\beta) sc(\psi) & r_{bp} c^2(\beta) s(\psi) \\ c^2(\beta) c^2(\psi) & r_{bp} sc(\beta) sc(\psi) & r_{bp} sc(\beta) c^2(\psi) & r_{bp} c^2(\beta) c(\psi) & \\ r_{bp}^2 s^2(\beta) s^2(\psi) & r_{bp}^2 s^2(\beta) sc(\psi) & r_{bp}^2 s^2(\beta) sc(\psi) & r_{bp}^2 sc(\beta) s(\psi) & \\ r_{bp}^2 s^2(\beta) c^2(\psi) & r_{bp}^2 sc(\beta) c(\psi) & r_{bp}^2 c^2(\beta) & & \\ sym. & & & & r_{bp}^2 c^2(\beta) \end{bmatrix} \quad (13)$$

$$[K_{pg}] = \begin{bmatrix} -c^2(\beta) s^2(\psi) & -c^2(\beta) sc(\psi) & r_{bg} sc(\beta) s^2(\psi) & r_{bg} sc(\beta) sc(\psi) & r_{bg} c^2(\beta) s(\psi) \\ -c^2(\beta) sc(\psi) & -c^2(\beta) c^2(\psi) & r_{bg} sc(\beta) sc(\psi) & r_{bg} sc(\beta) c^2(\psi) & r_{bg} c^2(\beta) c(\psi) \\ -r_{bp} sc(\beta) s^2(\psi) & -r_{bp} sc(\beta) sc(\psi) & r_{bp} r_{bg} s^2(\beta) s^2(\psi) & r_{bp} r_{bg} s^2(\beta) sc(\psi) & r_{bp} r_{bg} sc(\beta) s(\psi) \\ -r_{bp} sc(\beta) sc(\psi) & -r_{bp} sc(\beta) c^2(\psi) & r_{bp} r_{bg} s^2(\beta) sc(\psi) & r_{bp} r_{bg} s^2(\beta) c^2(\psi) & r_{bp} r_{bg} sc(\beta) c(\psi) \\ -r_{bp} c^2(\beta) s(\psi) & -r_{bp} c^2(\beta) c(\psi) & r_{bp} r_{bg} sc(\beta) s(\psi) & r_{bp} r_{bg} sc(\beta) c(\psi) & r_{bp} r_{bg} c^2(\beta) \end{bmatrix} \quad (14)$$

$$[K_{gp}] = [K_{pg}]^T \quad (15)$$

$$[K_{gg}] = \begin{bmatrix} c^2(\beta) s^2(\psi) & c^2(\beta) sc(\psi) & -r_{b_g} sc(\beta) s^2(\psi) & -r_{b_g} sc(\beta) sc(\psi) & -r_{b_g} c^2(\beta) s(\psi) \\ c^2(\beta) c^2(\psi) & -r_{b_g} sc(\beta) sc(\psi) & -r_{b_g} sc(\beta) c^2(\psi) & -r_{b_g} c^2(\beta) c(\psi) \\ r_{b_g}^2 s^2(\beta) s^2(\psi) & r_{b_g}^2 s^2(\beta) sc(\psi) & r_{b_g}^2 sc(\beta) s(\psi) \\ r_{b_g}^2 s^2(\beta) c^2(\psi) & r_{b_g}^2 sc(\beta) c(\psi) \\ sym. & & & & r_{b_g}^2 c^2(\beta) \end{bmatrix} \quad (16)$$

where c indicates cosine, s indicates sine and sc indicates multiplication of sine and cosine of the same angle.

These partial matrix K_{pp} , K_{pg} , K_{gp} and, K_{gg} compose the mesh stiffness matrix of the finite element model, $[K_m]$, which of them in its equivalent degree of freedom. For example, if the degrees of freedom of the pinion are from 6 to 10 and the degrees of freedom of the gear are from 21 to 25, then $[K_m(6 : 10, 6 : 10)] = [K_{pp}]$, $[K_m(6 : 10, 21 : 25)] = [K_{pg}]$, $[K_m(21 : 25, 6 : 10)] = [K_{gp}]$ and $[K_m(21 : 25, 21 : 25)] = [K_{gg}]$.

4. RESULTS

A two-shaft geared rotor system was considered. Both shafts have only 3 nodes, with the bearings on the shafts ends and the discs at the central nodes. All shaft elements have length a 100 mm and diameter of 30 mm. All bearings have stiffness of $7 \cdot 10^7 N/m$ and damping of $150 Ns/m$, in both vertical and horizontal direction. Shafts have Young's modulus of $200 GPa$, shear modulus of $80 GPa$, density of $7800 kg/m^3$ and damping proportional to the stiffness by a coefficient of $3 \cdot 10^{-5}$. The pinion rotational speed is $500 rpm$. Numerical method to solve the equation of motion was Newmark-beta, with coefficients $\gamma = 0.5$ and $\beta = 0.25$. The time step was $10^{-5} s$.

In order to evaluate distinctions generated by different methods of mesh stiffness calculation, simulations were performed considering the system with a spur gear pair and with a helical gear pair, with helix angle (β) of 5° . The gear geometry is involute and teeth are standard. Other gears parameters are shown on Table 1.

Table 1. Simulation Data

Parameter	Pinion	Gear
Pressure angle [$^\circ$]	20	
Module [mm]	3	
Face width [mm]	20	
Number of teeth	25	30
Young Modulus [GPa]	200	200
Poisson's ratio	0.3	0.3

All methods explained in Section 2 were applied to calculate the mesh stiffness k_m , used in equation 10. The mean value of mesh stiffness necessary for step and sinusoidal function was the one obtained by API method. The Fourier expansion used to generate the sinusoidal function considered only one term ($i = 1$).

Figure 1 shows the comparison of mesh stiffness calculated for all considered methods, for both spur gear pair and helical gear pair. In both cases, API mesh stiffness value is underestimated, comparing to the mesh stiffness calculated by the variable cross section beam method. Since API is the mean value for step and sinusoidal function, these mesh stiffness are also underestimated.

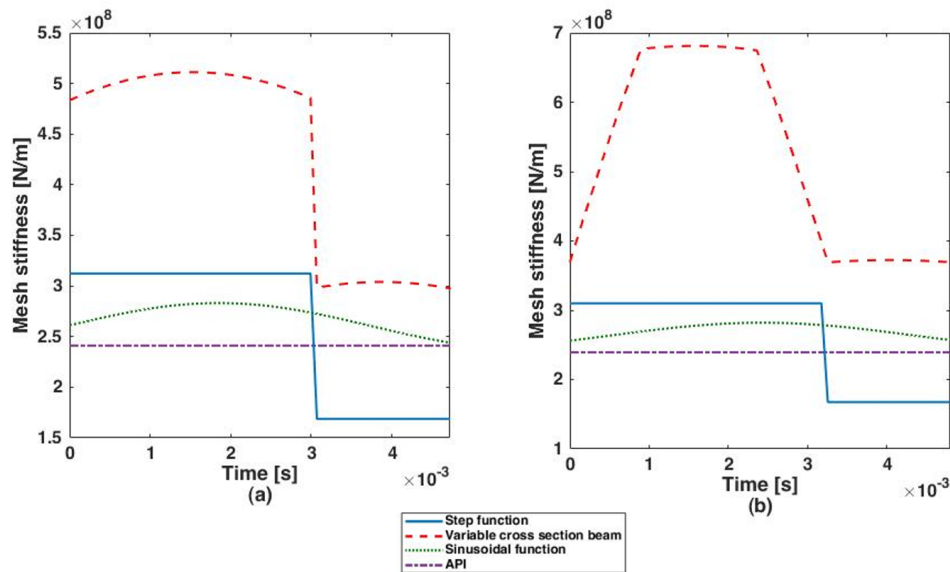


Figure 1. Comparison of calculated mesh stiffness for the (a) spur gear pair (b) helical gear pair.

Pinion horizontal displacement time response is presented in Figure 2. It also displays some details of transient and permanent response, and the differences on permanent response are more evident. To better understand these discrepancies, DFTs of permanent response were analysed (Figures 3-6). Mean value of all amplitudes is basically the same. Mesh stiffness is a parametric excitation and generates amplitude peaks on multiple frequencies of mesh frequency. As API provides a constant mesh stiffness, there are no amplitude peaks on higher order frequencies.

Comparison of displacements amplitudes of pinion and gear are shown in Figure 3 and Figure 4. Amplitude peaks of spur gears with sinusoidal-modeled mesh stiffness have nearly the same magnitude of beam-modeled mesh stiffness. In the case of helical gears, sinusoidal method peaks are lower than beam method peaks. Step method generates higher amplitudes in both cases, but this difference becomes more evident on the helical gear pair system response (graphics c and d). The same tendency occurs when considering the acceleration of the bearings on both shafts (Figures 5 and 6).

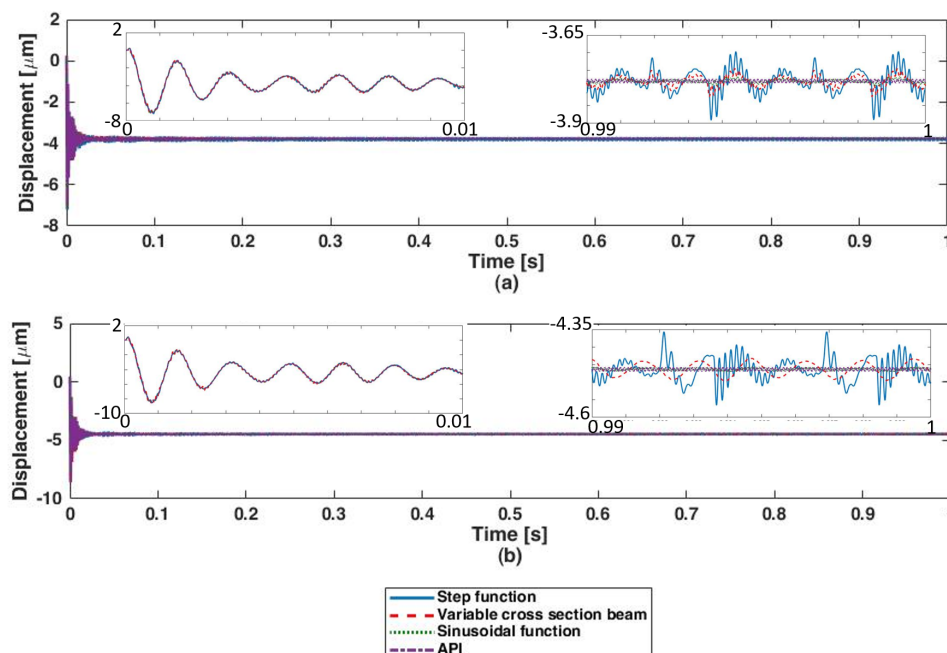


Figure 2. Comparison of pinion horizontal displacement time response (a) spur gear pair (b) helical gear pair.

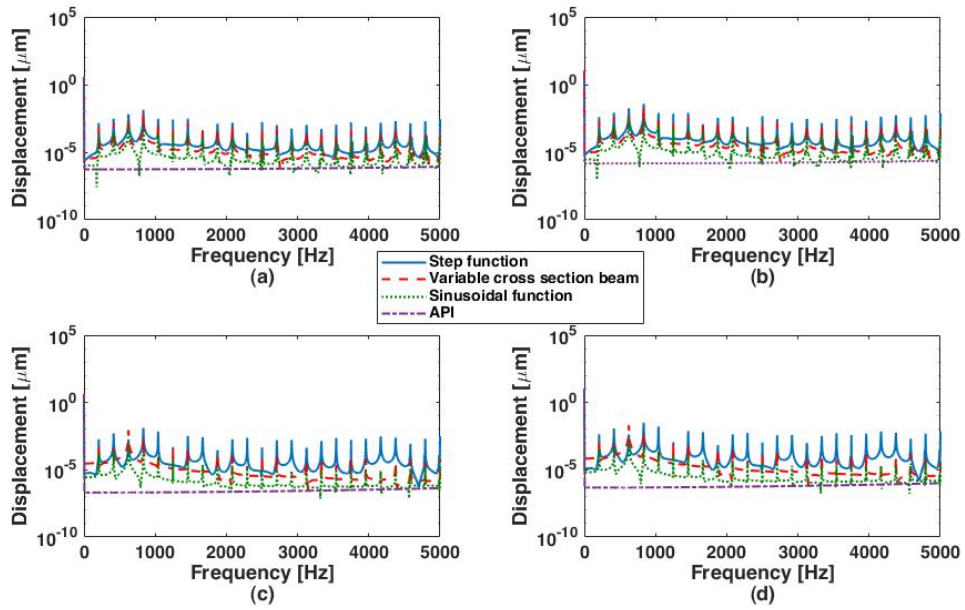


Figure 3. Comparison of displacements of gear 1 (a) horizontal direction, spur gear pair (b) vertical direction, spur gear pair (c) horizontal direction, helical gear pair (d) vertical direction, helical gear pair.

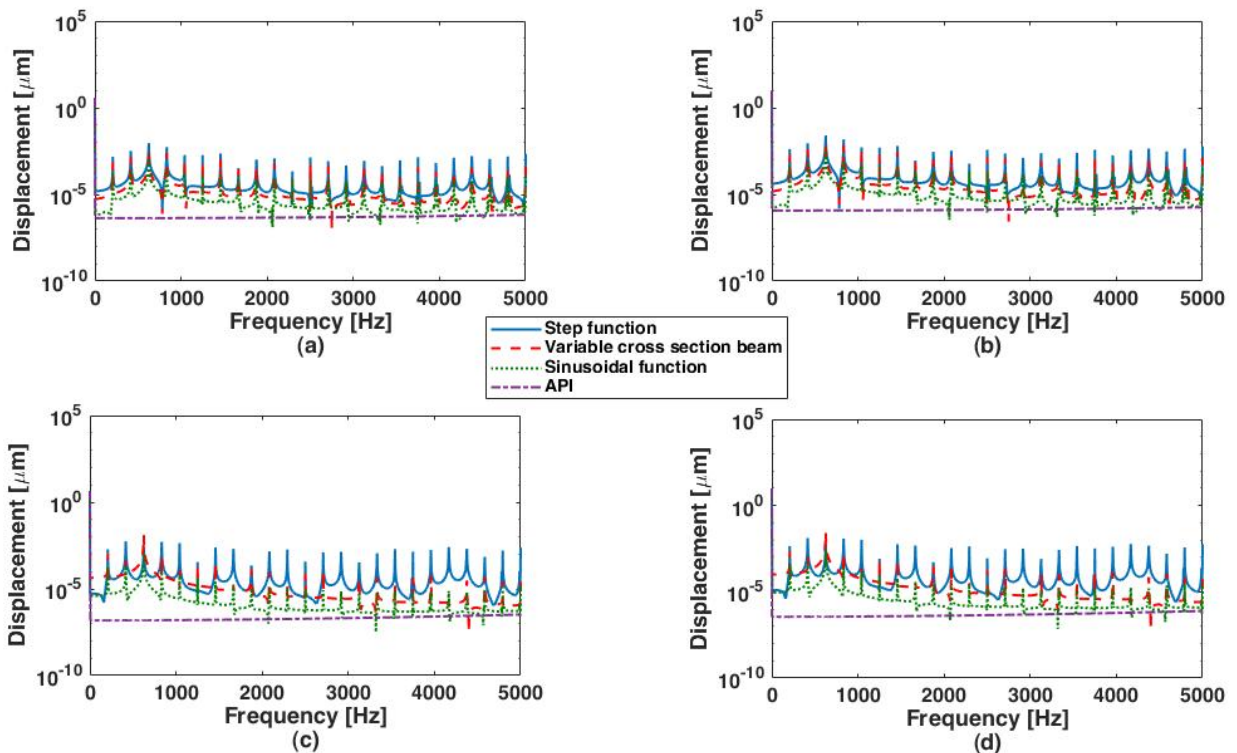


Figure 4. Comparison of displacements of gear 2 (a) horizontal direction, spur gear pair (b) vertical direction, spur gear pair (c) horizontal direction, helical gear pair (d) vertical direction, helical gear pair.

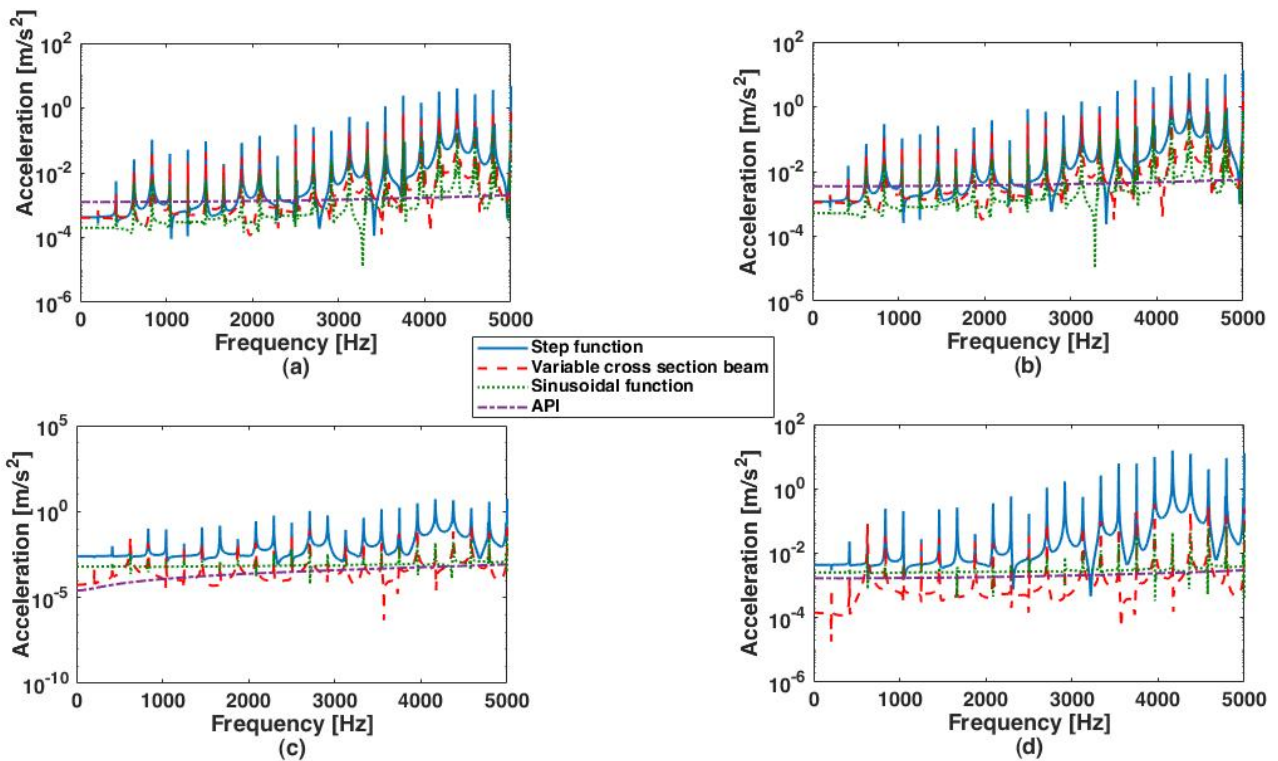


Figure 5. Comparison of accelerations of bearing 1, shaft 1 (a) horizontal direction, spur gear pair (b) vertical direction, spur gear pair (c) horizontal direction, helical gear pair (d) vertical direction, helical gear pair.

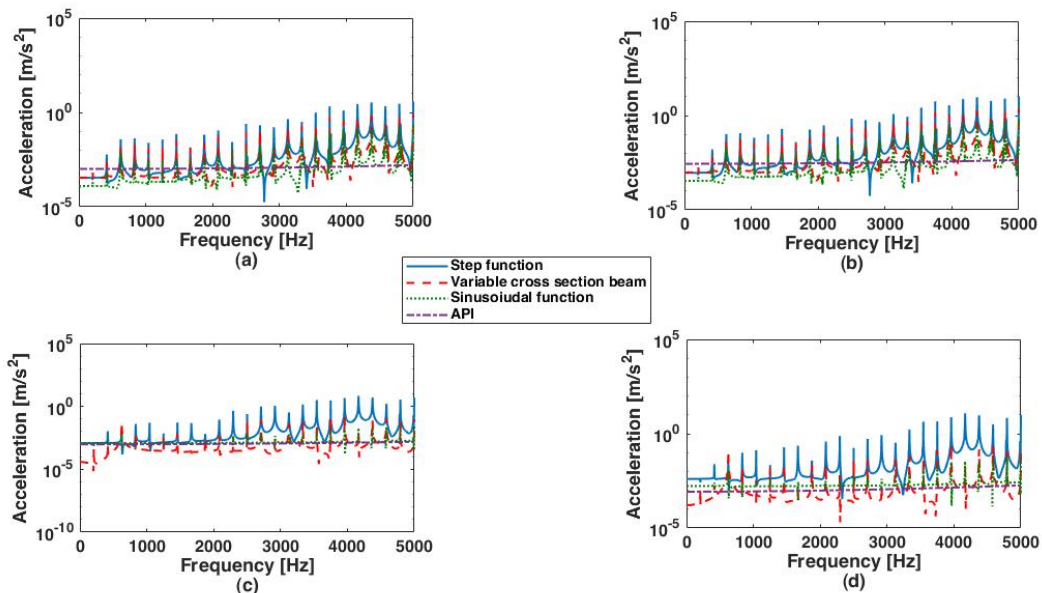


Figure 6. Comparison of accelerations of bearing 1, shaft 2 (a) horizontal direction, spur gear pair (b) vertical direction, spur gear pair (c) horizontal direction, helical gear pair (d) vertical direction, helical gear pair.

Differences on computational costs are irrelevant because the rotational speed was considered constant. In this case, beam method TVMS is calculated for only one time period, and replicated along all simulation time. If the rotational speed is no longer constant, mesh period changes along time and TVMS has to be calculated in each time step. In the case of beam method, angular position of gears also influence the mesh stiffness and, as the method depends on integrative operations, computational cost increases significantly.

Results presented on Figures 3 to 6 suggest that sinusoidal function underestimate system response, but the mean value considered to generate mesh stiffness was API. Figure 7 displays the comparison of the horizontal response of the bearing 1 assembled in shaft 1 for spur gear pair (a) and helical gear pair (b), considering TVMS calculated by beam method (red)

and by sinusoidal function (green) with mean value equal to beam method mean value. These results indicate that this approach causes an overestimation of response for the spur gear pair, but for the helical gear pair most amplitude peaks have nearly the same magnitude of the beam method peaks.

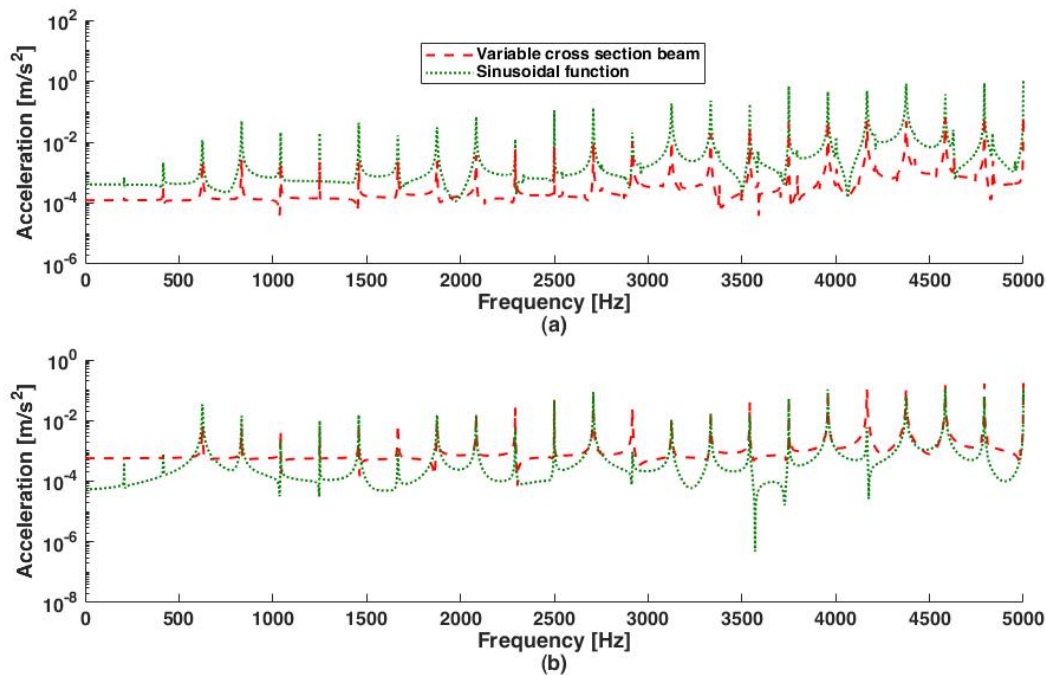


Figure 7. Comparison of horizontal accelerations of bearing 1, shaft 1 (a) spur gear pair (b) helical gear pair.

5. CONCLUSIONS

This paper intended to analyse the impact of different methods of mesh stiffness calculation on the dynamic response of a geared rotor. Four methods were considered: API, step function, sinusoidal function and variable cross section beam. Finite elements method was applied to model the 2-shaft rotating system. Both spur and helical gears were simulated in this rotor.

Variable cross section beam method provided a higher mean-value stiffness compared to API, for both spur and helical gear pair. Since API was used as a mean value for step and sinusoidal function, these methods presented also lower magnitudes of mesh stiffness, comparing to the beam method.

Rotor response with a API calculated mesh stiffness do not present amplitude peaks on multiple frequencies of the mesh period. This was expected because the method considers a constant mesh stiffness. The other methods consider the mesh period on their formulation.

Results indicate a tendency for the step function method generate higher amplitude peaks on the responses and for the sinusoidal function with API mean value generate slightly lower amplitude peaks, mostly for helical gears, compared to the variable beam method. Overestimation of amplitudes generated by the step function, specially on higher order frequencies, is greater in the helical gear pair response. Sinusoidal function with beam method mean value generates nearly the same results of beam method for the helical gear pair.

In conclusion, TVMS calculation methods are preferable than API method. For constant rotational speed simulations, it is recommended to calculate mesh stiffness by the mean method, because computational costs do not increase significantly and this method is the most precise one, because considers teeth geometry. In case of variable rotational speed, it is recommended to apply sinusoidal function with API mean value for the spur gear pair and with beam method mean value for the helical gear pair. Step function is not preferable comparing to sinusoidal function because it overestimates high frequency amplitudes of the response.

6. ACKNOWLEDGEMENTS

The authors would like to thank Petrobras Brazil and CAPES for providing financial support to this research.

7. REFERENCES

- API, 2005. "API Standard Paragraphs Rotordynamic Tutorial: Lateral Critical Speeds, Unbalance Response, Stability, Train Torsionals, and Rotor Balancing". Technical Report August 2005.
- Cooley, C.G., Liu, C., Dai, X. and Parker, R.G., 2016. "Gear tooth mesh stiffness: A comparison of calculation approaches". *Mechanism and Machine Theory*, Vol. 105, pp. 540–553. ISSN 0094114X. doi:10.1016/j.mechmachtheory.2016.07.021. URL <http://dx.doi.org/10.1016/j.mechmachtheory.2016.07.021>.
- Kahraman, A., Nevzatoguzven, H., Houser, D.R. and Zakrajsek, J.J., 1992. "Dynamic analysis of geared rotors by finite elements". *Journal of Mechanical Design, Transactions of the ASME*, Vol. 114, No. 3, pp. 507–514. ISSN 10500472. doi:10.1115/1.2926579.
- Kahraman, A. and Singh, R., 1991. "Non-Linear Dynamics With of a Geared Rotor-Bearing System". *Journal of Sound and Vibration*, Vol. 114, No. 3, pp. 469–506.
- Kim, W., Yoo, H.H. and Chung, J., 2010. "Dynamic analysis for a pair of spur gears with translational motion due to bearing deformation". *Journal of Sound and Vibration*, Vol. 329, No. 21, pp. 4409–4421. ISSN 0022460X. doi:10.1016/j.jsv.2010.04.026.
- Kubur, M., Kahraman, A., Zini, D.M. and Kienzle, K., 2004. "Dynamic analysis of a multi-shaft helical gear transmission by finite elements: Model and experiment". *Journal of Vibration and Acoustics, Transactions of the ASME*, Vol. 126, No. 3, pp. 398–406. ISSN 10489002. doi:10.1115/1.1760561.
- Ma, H., Song, R., Pang, X. and Wen, B., 2014. "Time-varying mesh stiffness calculation of cracked spur gears". *Engineering Failure Analysis*, Vol. 44, pp. 179–194. ISSN 13506307. doi:10.1016/j.engfailanal.2014.05.018. URL <http://dx.doi.org/10.1016/j.engfailanal.2014.05.018>.
- Meagher, J., Wu, X., Kong, D. and Lee, C.H., 2010. "A Comparison of Gear Mesh Stiffness Modeling Strategies Jim". In *Proceedings of the IMAC - XXVIII*. Jacksonville, Florida USA, Vol. 3, pp. 255–263. ISBN 978-1-4419-9834-7. doi:10.1007/978-1-4419-9834-7. URL <http://link.springer.com/10.1007/978-1-4419-9834-7>.
- Rao, J.S., Shiau, T.N. and Chang, J.R., 1998. "Theoretical analysis of lateral response due to torsional excitation of geared rotors". *Mechanism and Machine Theory*, Vol. 33, No. 6, pp. 761–783. ISSN 0094114X. doi:10.1016/S0094-114X(97)00056-6.
- Shin, D. and Palazzolo, A., 2020. "Nonlinear analysis of a geared rotor system supported by fluid film journal bearings". *Journal of Sound and Vibration*, Vol. 475, p. 115269. ISSN 10958568. doi:10.1016/j.jsv.2020.115269. URL <https://doi.org/10.1016/j.jsv.2020.115269>.
- Theodossiadis, S. and Natsiavas, S., 2001. "On geared rotordynamic systems with oil journal bearings". *Journal of Sound and Vibration*, Vol. 243, No. 4, pp. 721–745. ISSN 0022460X. doi:10.1006/jsvi.2000.3430.
- Wan, Z., Cao, H., Zi, Y., He, W. and Chen, Y., 2015. "Mesh stiffness calculation using an accumulated integral potential energy method and dynamic analysis of helical gears". *Mechanism and Machine Theory*, Vol. 92, pp. 447–463. ISSN 0094114X. doi:10.1016/j.mechmachtheory.2015.06.011. URL <http://dx.doi.org/10.1016/j.mechmachtheory.2015.06.011>.
- Wygant, K., Robertson, C., Li, F., 2018. "Tutorial: Rotor Bearing Dynamics of Integrally Geared Turbomachinery". In *Asian Turbomachinery & Pump Symposium*. Singapore.
- Yi, Y., Huang, K., Xiong, Y. and Sang, M., 2019. "Nonlinear dynamic modelling and analysis for a spur gear system with time-varying pressure angle and gear backlash". *Mechanical Systems and Signal Processing*, Vol. 132, pp. 18–34. ISSN 10961216. doi:10.1016/j.ymsp.2019.06.013. URL <https://doi.org/10.1016/j.ymsp.2019.06.013>.

8. RESPONSIBILITY NOTICE

The authors are solely responsible for the printed material included in this paper.